Critical state based trends for the monotonic response of mine tailings

Luis Vergaray & Jorge Macedo Georgia Institute of Technology, Atlanta, Georgia, USA

ABSTRACT: Static liquefaction has been associated with numerous recent failures of tailings storage facilities (TSFs) around the world (e.g. the 2019 Brumadhino failure in Brazil). These failures lead to devastating consequences for the environment and civil infrastructure and lead to loss of human lives. Static liquefaction is just another facet of soil behavior under monotonic loadings, and hence it should be explained under a mechanistic framework. In this study, we present trends for the response of mine tailings to monotonic loading considering a) triaxial tests, b) bender element tests, and c) consolidation tests performed on 53 mine tailings materials (including recent case histories). These materials have a broad range of states, a range of particle size distributions (from silty sand to almost pure silt mine tailings), and a broad range of compressibility. The trends are evaluated in the context of static liquefaction using critical state soil mechanics concepts and considering different state definitions. In particular, we present trends for shear strength (residual and peak), state and brittleness soil indexes, excess pore pressure indexes and dilatancy. Finally, static liquefaction screening indexes are proposed based on the observed trends.

1 INTRODUCTION

The static liquefaction of mine tailings has caused numerous recent failures, e.g., the 2014 Mount Polley disaster in Canada (Morgenstern et al., 2015), the 2015 Fundao failure in Brazil (Morgenstern et al., 2016), the 2018 Cadia failure in Australia (Morgenstern et al., 2019), and the 2019 Brumadhino failure in Brazil (Robertson et al., 2019). Such failures of tailings storage facilities (TSFs) have caused unprecedented devastating consequences for the environment, infrastructure damage as well as human losses. These failures have triggered international debates regarding the safety of TSF systems. In particular, the conditions that result in static liquefaction of mine tailings remain a considerable concern affecting the financial viability of mines and the willingness of governments to allow mining.

In the U.S. exist approximately 1200 TSFs, with 60% of them having a significant hazard according to the USACE classification (USACE, 2016). Hence, the safety of TSFs is an important issue. As engineering practice is moving more towards finite element or finite difference-based stress analyses (e.g., the evaluations performed in the forensic studies after recent failures), understanding the mechanical response of mine tailings is also fundamental for the calibration of constitutive models that can later be used in numerical simulations. This is not simple because mine tailings are often characterized as intermediate materials (pure silts or sandy silts), which represents a fundamental challenge for understanding their mechanical response. Tailings are also geologically young materials, with angular grains rather than subrounded and often with lower proportions of quartz than many natural soils; thus, standard geotechnical correlations should not be taken as applicable to tailings without detailed consideration of these factors.

Previous efforts on understanding the trends in the mechanical response of particulate materials under monotonic loadings have been mainly focused on sands with low fine contents (e.g., Sadre-karimi, 2014; Jefferies & Been, 2016, Rabbi et al., 2019). In terms of mine tailings, the experimental studies that have evaluated their mechanical response and the associated mechanical parameters are somewhat limited compared to sand materials (e.g., Jefferies & Been, 2016; Shuttle & Jefferies, 2016; Fourie & Tshabalala, 2005; Carrera et al., 2011). In this study, we present trends for mechanical-based parameters that control the response of mine tailings, in the context of static liquefaction, which have not been previously explored considering a large set of tailings materials. The trends are presented using results from 53 mine tailings materials (including available data from the recent failures previously discussed), which have been processed in a uniform manner.

2 DATABASE

The whole database consists has 53 different mine tailings material, 7 of them were generated as part of this study and the rest were compiled from Shuttle & Cunning (2007), Anderson & Eldridge (2011), Bedin et al. (2012), Schnaid et al. (2013), Been (2016), Li & Coop (2018), Li & Coop (2019), Raposo (2016), Torres (2016), Morgenstern et al. (2016), Riemer et al. (2017), Li (2017), Robertson et al. (2019), Macedo & Petalas (2019), Gill (2019), Reid & Fanni (2020), Reid et al. (2018), Reid et al. (2020), Fourie & Papageorgiou(2001), and Carrera (2011). The mine tailings database corresponds to different ores (i.e., gold, iron, silver, copper, zinc, platinum) covering a broad range of fine contents (FC = 0 - 100 %), initial confining stress (20 - 6000 kPa), specific gravity (Gs = 2.63 - 4.89), and states (i.e., very loose to dense). The following properties were evaluated for each material: the critical state line (CSL), the stress ratio at critical state (M_{tc}), the state-dilatancy parameter (χ), the stiffness-confinement dependence parameters (A, B) according to $G = A.F(e).(p/p_a)^B$, where F(e) represent the functional form proposed by Hardin & Richart (1963) and Pestana & Whittle (1995). Figure 1 shows the particle size distribution for the materials considered in this study, separating them by fine contents for easier visualization. Additional details are provided in Macedo and Vergaray (2021).

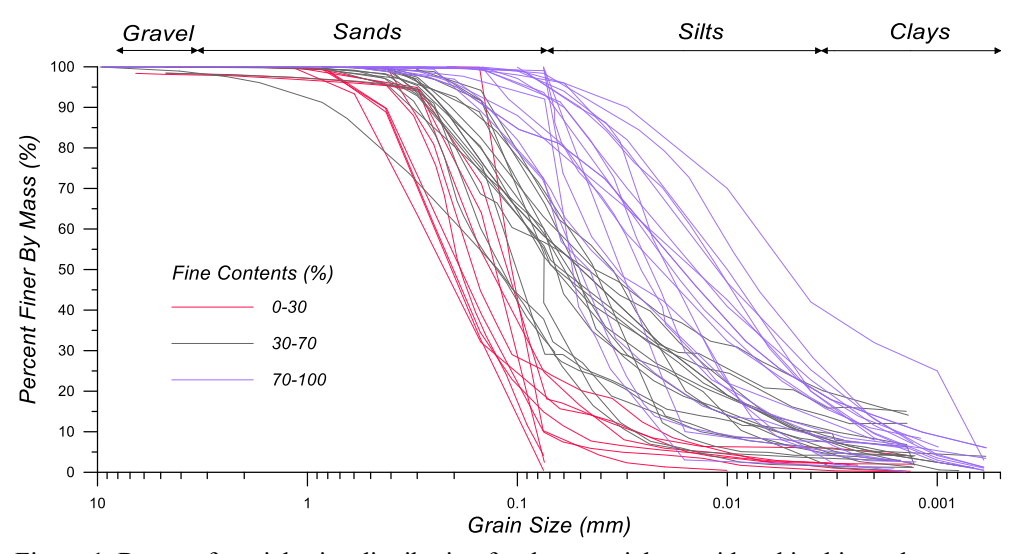


Figure 1. Range of particle size distribution for the materials considered in this study.

It is important to highlight that Γ , λ_e , M_{tc} , N, χ , A, and B are often present as parameters in robust constitutive models, usually formulated for sands (although often named differently or represented by other proxies), and are the basis for the current mechanical-based understanding of static liquefaction. Figure 2 shows an example of the calculation of these parameters for material 12. Figure 2a shows the estimation of the CSL, Figure 2b shows the η_{max} versus D_{min} plot to estimate M_{tc} and N, Figure 2c shows the state-dilatancy relationship to estimate χ , and Figure 2d shows the G versus P plot to estimate P and P and P and P and P and P are P and P and P and P and P are P and P and P are P and P and P are often are P and P are often are often are of the current mechanical-based understanding of static liquefaction.

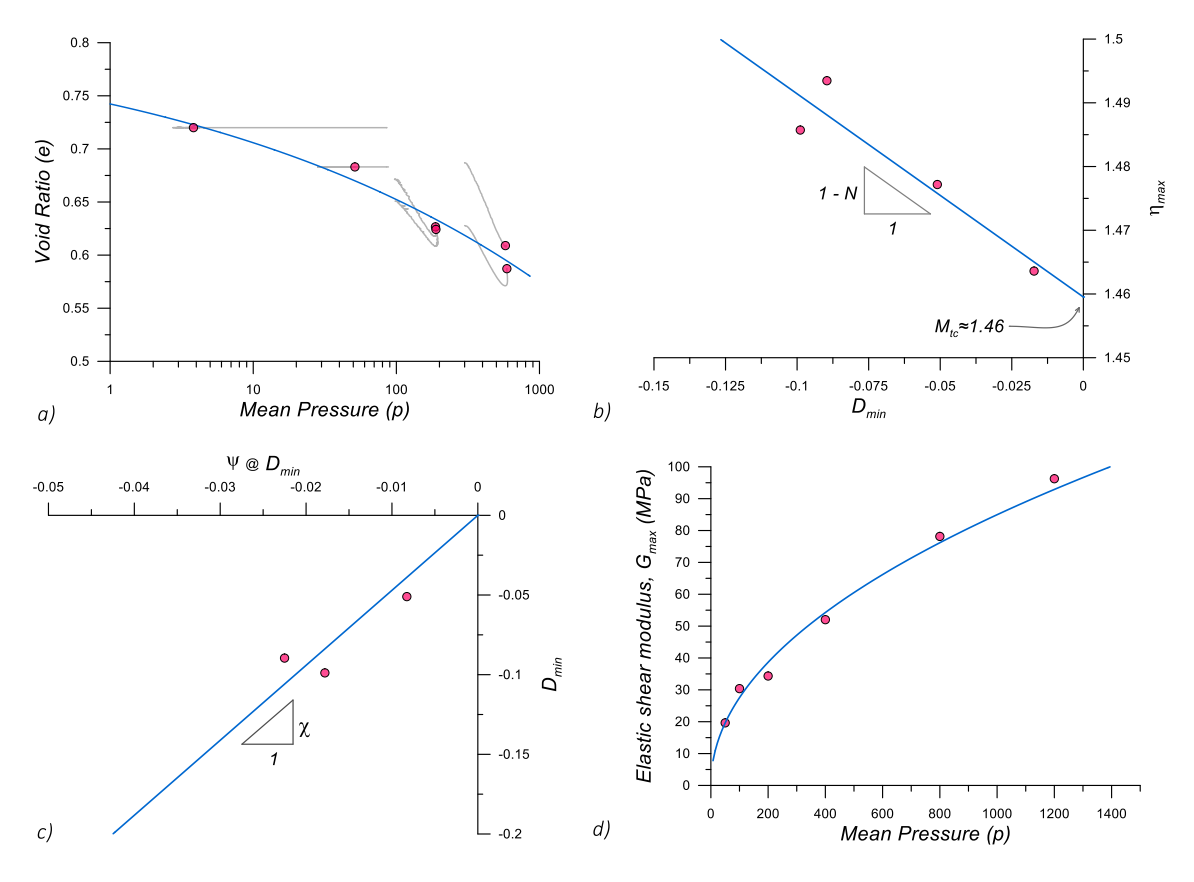


Figure 2. Illustration of the estimation of mechanical-based parameters consistent with the critical state theory for material 12. a) CSL estimation, b) η_{max} versus D_{min} plot to estimate M_{tc} and N, c) state-dilatancy relationship to estimate χ , and d) G versus p plot to estimate Λ , and Π .

3 TRENDS IN THE MECHANICAL RESPONSE OF MINE TAILINGS

3.1 Critical state parameters and stiffness

Figure 3a shows the distribution of the CSLs for all the materials considered in this study; it can be observed that the estimated CSLs were, in most cases, followed a linear relationship (in a Semi-Log space). In addition, the estimated CSLs cover a broad spectrum in the e versus p plane (the maximum difference in e for a given p is in the order of 0.55). Figure 3b illustrates the spectrum of the maximum shear modulus (G) variation (i.e., G versus mean pressure) estimated through bender element tests considering a broad range of densities.

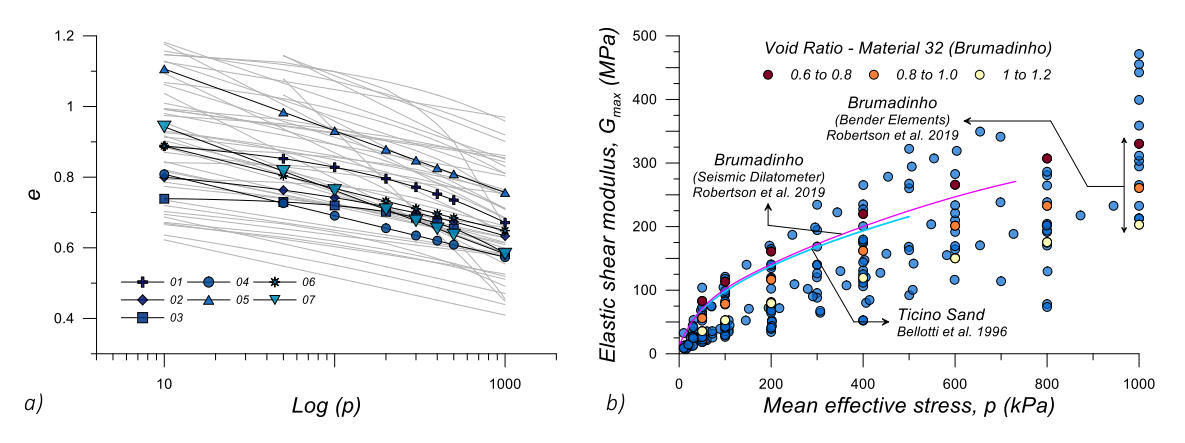


Figure 3. a) Variation of ψ and D_{min} for sands and mine tailings. b) Variation of χ and C_u/D_{50}

3.2 Stiffness

Figure 4a shows a histogram of M_{tc} values for tailings materials sand materials. The M_{tc} values for sand materials were obtained from Jefferies & Been (2016). It can be observed that M_{tc} values for mine tailings are generally larger compared to sands, which has also been observed in previous studies (e.g., Reid, 2015). This is due to the angularity associated with mine tailings as a product of the mineral processing. Figure 4b and 4c, show histograms for the A and B coefficients in Equation 2. It can be observed that the A coefficient typically varies from 10 Mpa to 60 Mpa, whereas the variation of B is generally between 0.4 and 0.7. To better understand the variation of the A coefficient, we plotted A versus the initial state parameter in Figure 4d, which suggested a good correlation.

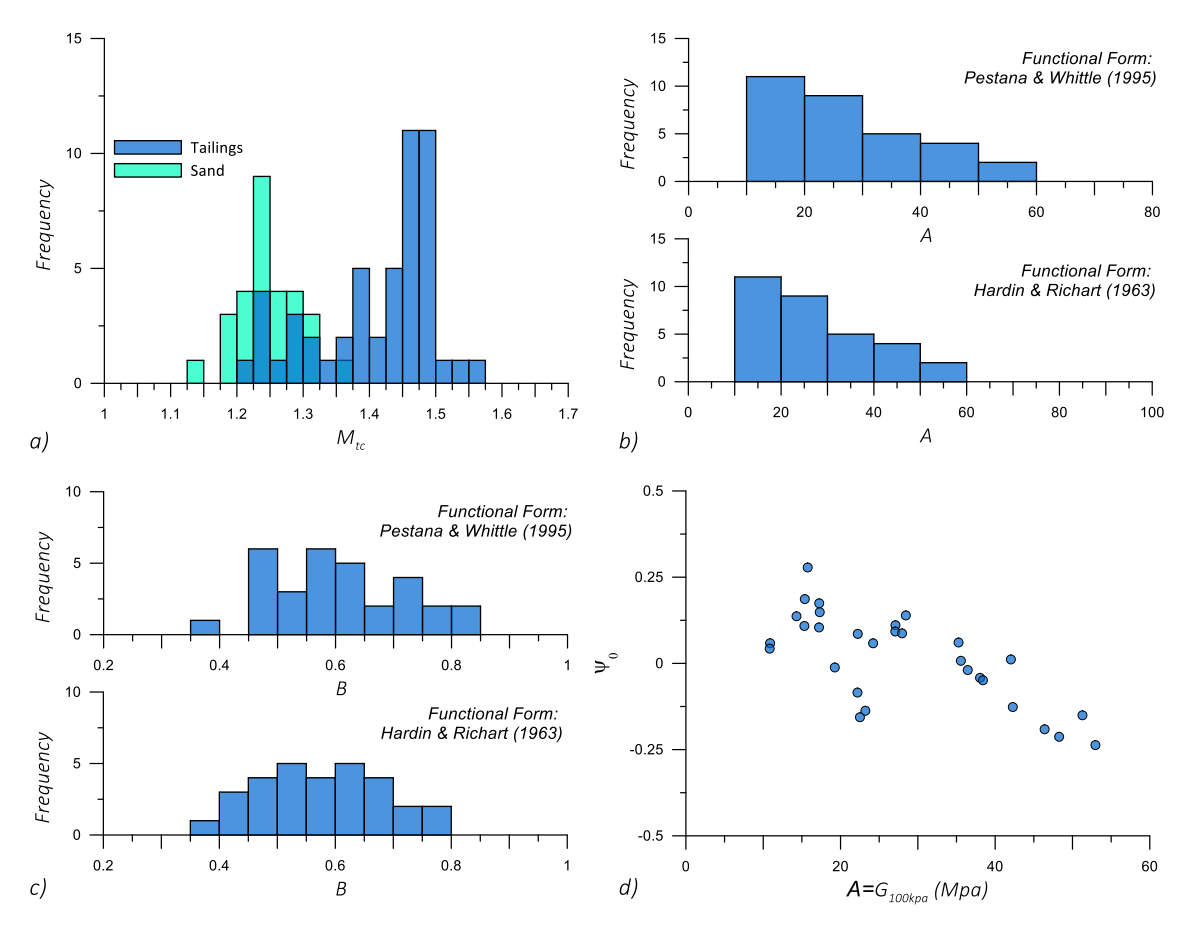


Figure 4. a) Distribution of M_{tc} values for tailing and sand materials, b), c) distribution of the A and B parameters in Equations 3a, and 3b, respectively, and d) A versus state parameter variation.

3.3 Residual and peak strength

In the following figures (Fig. 5 to 6) we discuss trends in terms of peak and residual shear strengths. Figure 5a and 5b shows the variations of Su_r/σ'_0 and Su_Y/σ'_0 in terms of I_b , along with upper and lower bound trends for sand materials extracted from Sadrekarimi (2014). It is noticed that, in general, the trends are reasonably consistent. Figure 5c shows the variation of Su_r/σ'_0 in terms of ψ_0 along with similar trends for sands with different compressibility (including the Lagunillas sandy silt) extracted from Sadrekarimi (2013). Figure 5d shows the variation of Su_Y/σ'_0 in terms of and ψ_0 along with upper and lower bound trends for Su_Y/σ'_0 in sands extracted from Jefferies & Been (2016).

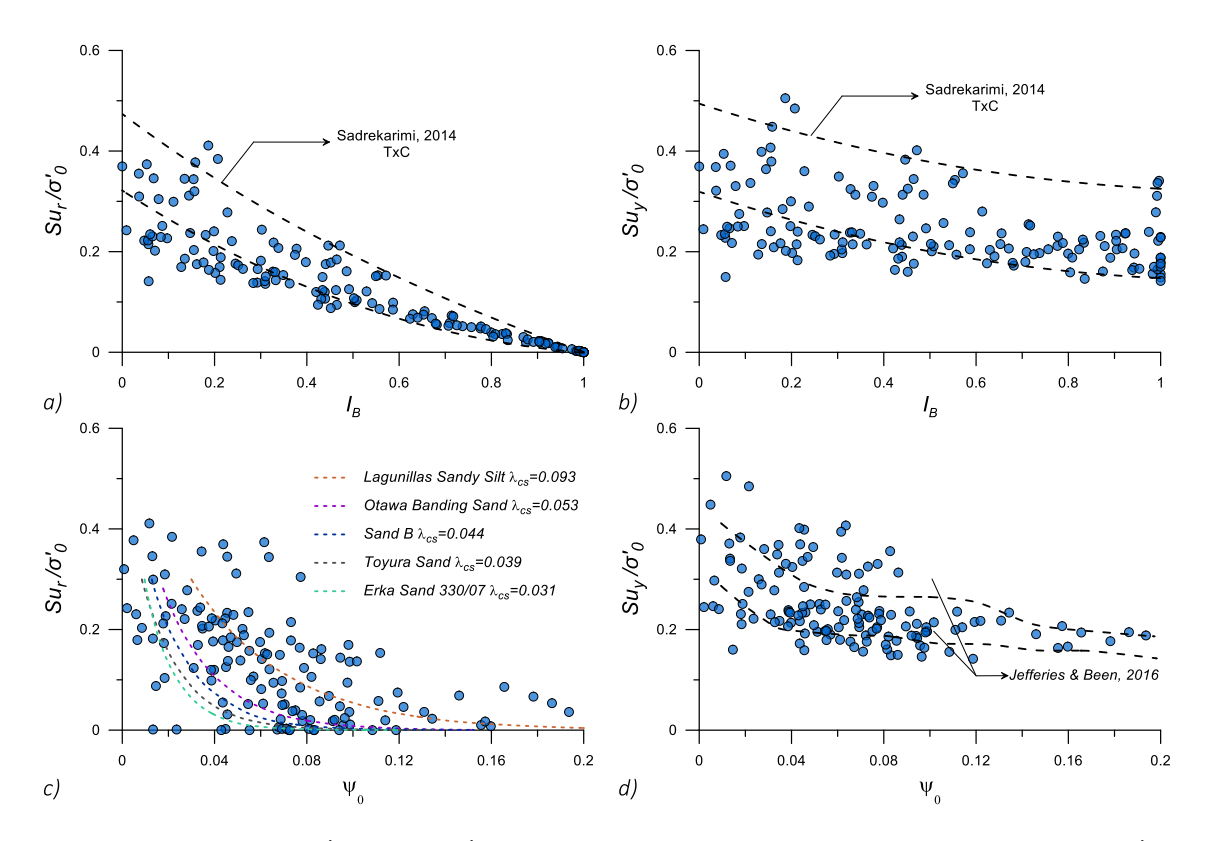


Figure 5. Variation of Su_r/σ'_0 and Su_r/σ'_0 vs the brittleness index ((a) and (b), respectively); and Su_r/σ'_0 and Su_r/σ'_0 vs the initial state parameter (ψ_0) ((c) and (d), respectively).

The variation of Su_Y/σ'_0 in Figure 5c suggests that Su_Y/σ'_0 tends to be larger in mine tailings compare to the sands in Jefferies & Been (2016) when ψ is lower than 0.1. To bring the effects of compressibility, we normalized the state parameter by λ_e . This normalization may also cancel out some fabric-related effects as compressibility is expected to be influenced by fabric.

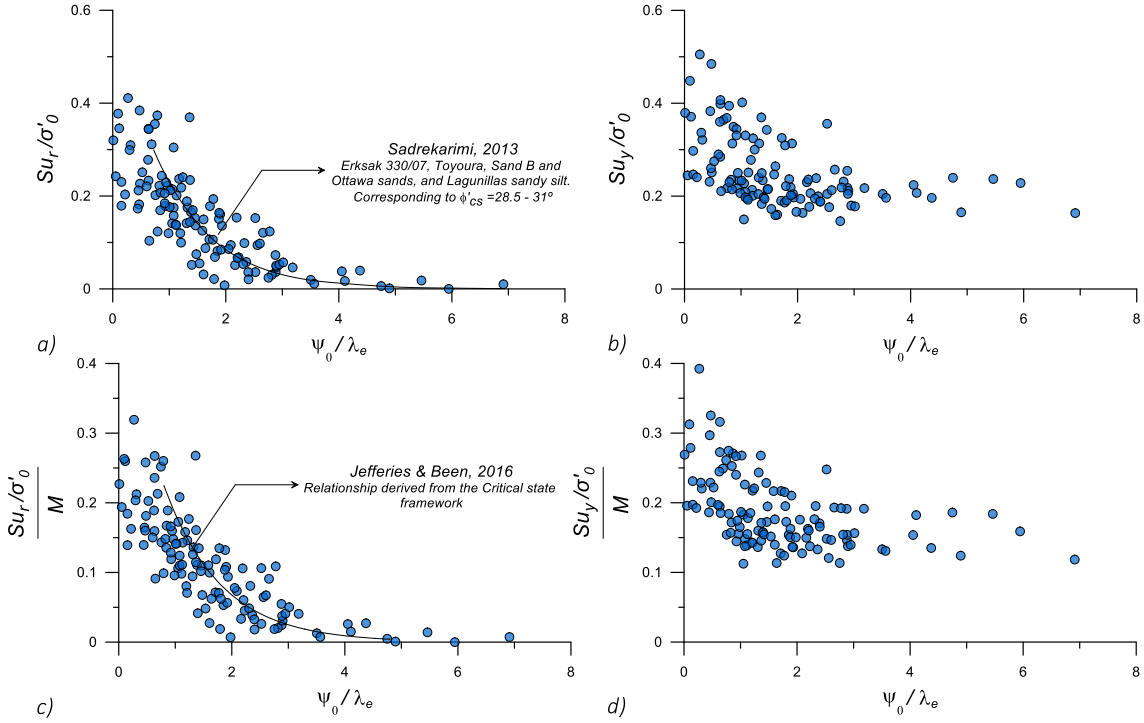


Figure 6. Variation of Su_r/σ'_0 and Su_r/σ'_0 versus ψ_0/λ_e ((a) and (b), respectively); and $Su_r/(M_{tc}\sigma'_0)$ and $Su_r/(M\sigma'_0)$ versus ψ_0/λ_e ((c) and (d), respectively).

Figure 6a and 6b shows the variation of Su_r/σ'_0 and Su_Y/σ'_0 versus ψ/λ_e , now it can be observed that bringing λ_e decreases the variability in the trends, and the normalized trends for mine tailings are now more consistent with those for sand materials reported by Sadrekarimi (2013). Besides, in Figure 6c and 6d to account for the effects of angularity in strength, we further normalized the Su_r/σ'_0 by M_{tc} , and plotted the results in terms of ψ/λ_e . Recall that from CSSM concepts (e.g., Jefferies & Been, 2016) $Su_r/(M\sigma'_0) = 0.5exp(-\psi/\lambda_e)$, which is also plotted in Figure 6c.

3.4 State and brittleness soil indexes

Figure 7a to 7d show the relationship between different parameters to represent the state and brittleness of a soil material. In these figures, the flow liquefaction cases that correspond to full softening and partial softening are presented in red and yellow colors, respectively Figure 7a shows the relationship between I_b and ψ/λ_e , along with the data from Smith et al. (2019), and the upper and lower bounds proposed by them for contractive materials (i.e., $\psi > 0$). It can be observed that our data is consistent with these upper and lower bounds. Of note, the trends suggest that flow liquefaction cases with partial softening may have in general a I_b larger than 0.25 and a ψ/λ_e larger than 0.75, whereas the flow liquefaction cases with full softening may be associated with I_b values higher than 0.6 and ψ/λ_e values larger than 1.5. Figure 7b shows the relationship between I_b and I_P . As expected I_P increases with the increase of I_b , and I_P values higher than 2.5 seem to be indicative of flow liquefaction with partial softening, whereas values larger than 10 may be indicative of potential flow liquefaction with full softening. Figure 7c shows the variation of ψ/λ_e and I_P , suggesting a good correlation between these parameters until flow liquefaction with full softening occurs in cases with $\psi/\lambda_e>3$. Finally, Figure 7d shows the variation of ψ_m and ψ/λ_e , again a good correlation is observed until $\psi/\lambda_e > 3$. Interestingly, ψ_m alone brings comparable information as ψ/λ_e because it also includes information on the state pressure index.

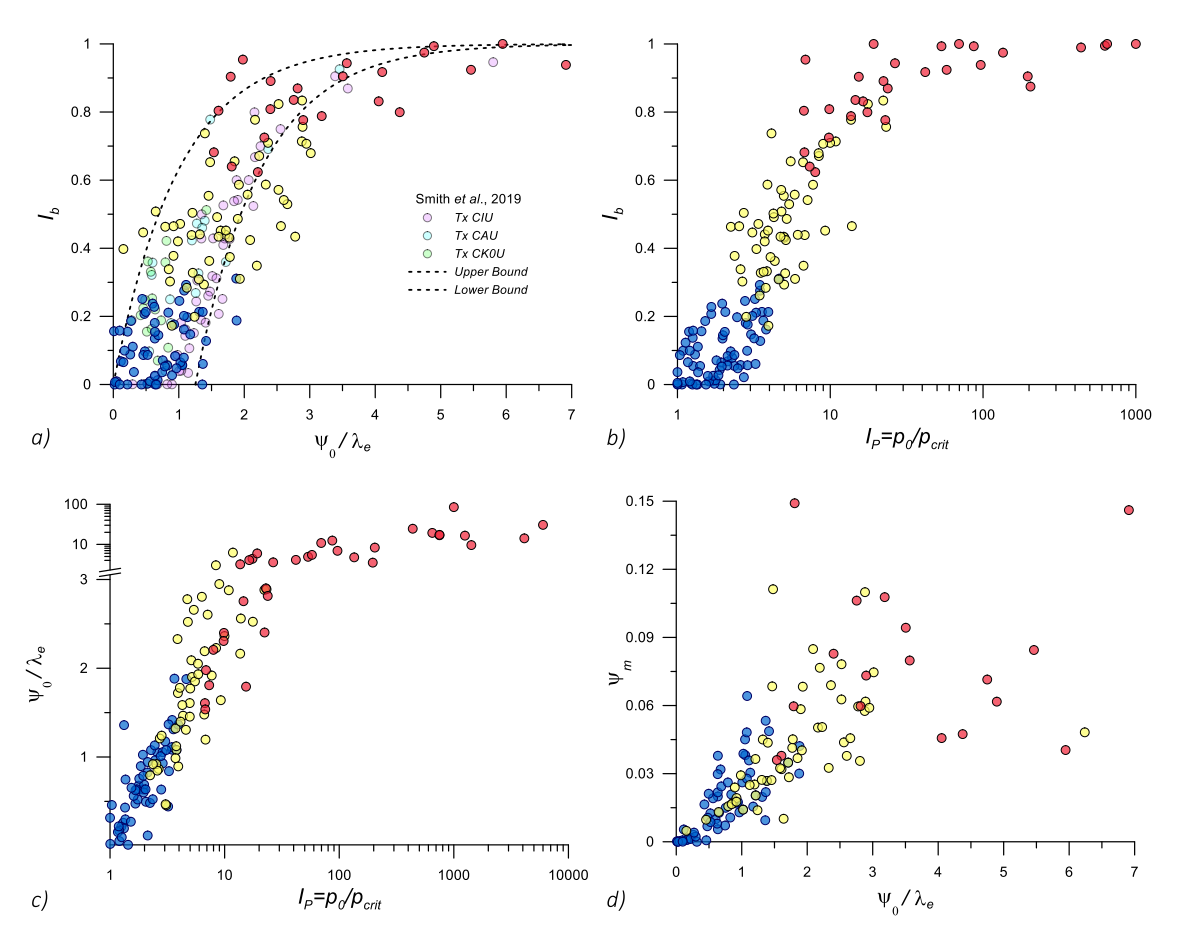


Figure 7. a) Relationship between I_b and ψ/λ_e , b) I_b versus I_p , c) ψ/λ_e versus I_p , and d) ψ_m versus ψ/λ_e .

3.5 Excess pore pressures

Figure 8a shows the variation of $r_u = \Delta u/\sigma'_0$ versus I_b along with the trend of r_u relationships for sands considering triaxial extension (TxE), plane strain compression (PSC), and triaxial compression (TxC) conditions. The TxE and PSC trends were extracted from Sadrekarimi (2016), and the TxC trends were extracted from Sadrekarimi (2020). In general, it can be observed that flow liquefaction cases (partial and full softening) show r_u values large than 0.8, and the data is generally consistent with the average trend extracted for sand materials, but it is observed that the r_u values in mine tailings tend to be larger compared to sands in cases with partial softening. Figure 8b shows the r_u variation in terms of ψ . In general, large r_u values were observed with most values higher than 0.6 for $\psi > 0$. As expected r_u increases with the increase in r_u and r_u higher than 0.1 or a r_u higher than 0 are indicative or large excess pore pressure generation (i.e., $r_u > 0.6$).

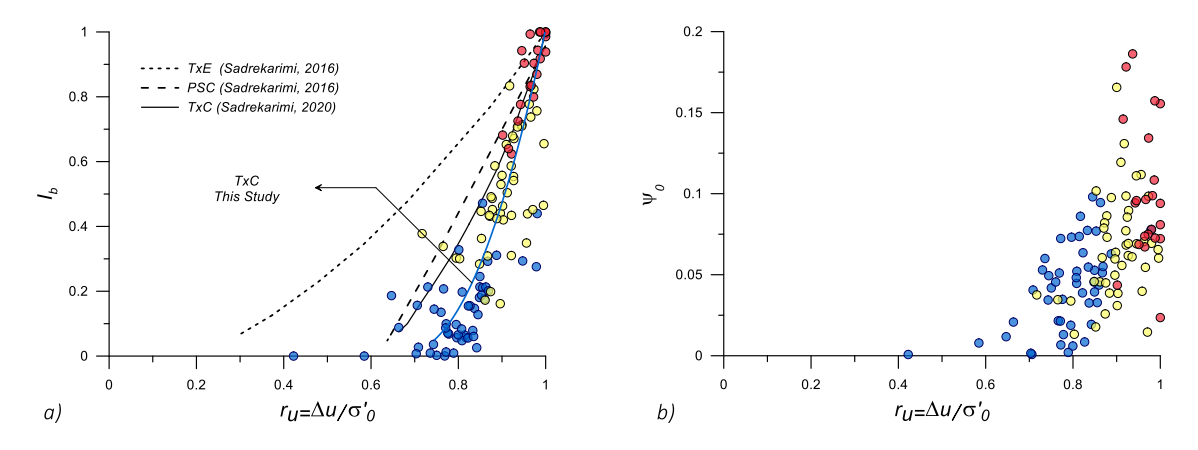


Figure 8. Variation of r_u vs a) the brittleness index, and b) the initial state parameter ψ_0 .

3.6 Dilatancy

Figure 9a shows the variation of the maximum dilatancy in triaxial CD tests versus ψ_0 , considering the mine tailings from this study and data available in Jefferies & Been (2016) for sand materials. If we fit the data to the relationship suggested by Been & Jefferies (1985), given by $D_{min} = \chi \psi$ we obtain representative χ values of 3.0 for sands, and 4.0 for tailings. This suggests that mine tailings have an average stronger scaling of dilatancy compared with sands, given a similar state parameter. This can be explained considering that χ can be though as a kinematic parameter related to the potential of particulate materials to re-accommodate particles. Given the more angularity of mine tailings compared to sands, mine tailings seem to have, on average, a higher potential on re-accommodating particles.

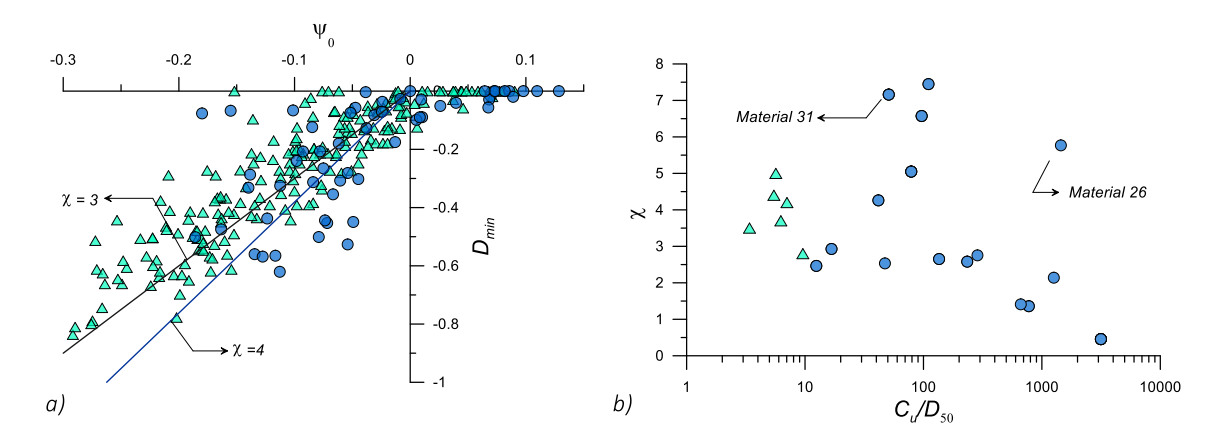


Figure 9. a) Variation of ψ and D_{min} for sands and mine tailings. b) Variation of χ and C_u/D_{50}

Figure 9b shows the variation of χ and C_u/D_{50} for mine tailings and some well-known sand materials (i.e., Erksak, Braster, Changi, Fraser, Nerlek, and Ticino sands). The data for sands was obtained from Jefferies & Been (2016). It can be observed that the χ values in sands vary in a narrow range between 3.5 and 5.0, which correspond to C_u and C_u/D_{50} values that are also in a narrow range (1 to 3, and 3 to 10, respectively). In the case of mine tailings, we observe that χ tends to decrease with the increase of C_u/D_{50} , which is consistent with observations from DEM simulations (Yan & Dong, 2011). We also noticed that the lowest χ values (lower than 1.4) correspond to materials with large FC (larger than 85%) and important clay size fractions. This observation is consistent with the findings from (Cola & Simonini, 2002). The materials 26 and 31 (which correspond to the Cadia and Brumadinho failures previously discussed) showed large χ values (5.8 and 7.2, respectively). These large values may be associated with the large angularity on these materials, and bonding effects, as suggested by Robertson et al. (2019) based on inspections of scanning electron microscope (SEM) images from the Brumadinho tailings.

4 CONCLUSIONS

In this study, we have used critical state soil mechanics (CSSM) concepts to examined salient trends on the mechanical response of mine tailings in the context of static liquefaction, highlighting the role the relative proportions of different particles sizes, and particle properties. Our results suggest that mine tailings fit the same framework as natural sands, with the key difference of showing a much larger M_{tc} and somewhat larger χ , both attributed to underlying particle shape, which then affects standard correlations. Thus, the mechanical response of mine tailings can be reasonably well explained once CSSM-based parameters such as Γ , λ_e , ψ , M_{tc} , χ , N, and G are incorporated.

Additional salient conclusions from this study include:

- The M_{tc} values in mine tailings (in the order of 1.4) are larger, on average, compared to M_{tc} values on natural sands (in the order of 1.2). This is associated to the particle shape of mine tailings, which tend to have more angular particles compared to the subrounded grains found in natural soils.
- Using the functional forms from Hardin & Richart (1963) and Pestana & Whittle (1995) for G (Equation 3), we observed that the parameter A that controls the magnitude of G correlates well with ψ_0 . In addition, the parameter B that controls the dependence on p, generally varies from 0.4 to 0.8.
- Compressibility can have an important effect on Su_r/σ'_0 , and also controls Su_y/σ'_0 . Hence, it should be carefully considered in evaluating appropriate Su_r/σ'_0 and Su_y/σ'_0 design values.
- In general, we observed that the state and brittleness indexes considered in this study such as ψ_0 , ψ_m , ψ_v , I_P , I_b are correlated.
- The trends suggest that flow liquefaction cases with partial softening may have in general I_b , ψ/λ , and I_P values larger than 0.25, 0.75, and 2.5, respectively. Whereas flow liquefaction with full softening is associated with I_b , ψ/λ , and I_P values higher than 0.6, 1.5, and 10, respectively. We recommend using these values as part of screening procedures in engineering practice.

5 ACKNOWLEDGEMENTS

This study has been funded by the National Science Foundation (NSF) under the CMMI 2013947 project and has also received support from the TAilings and IndustriaL waste ENGineering Center (TAILENG). We also thank Mr. Terry Eldridge, Mr. Mike Jefferies, and Dr. Li Wei, who kindly share data on mine tailings and sand materials.

- Anderson, C. & Eldridge, T. 2011. Critical state liquefaction assessment of an upstream constructed tailings sand dam. *Tailings and Mine Waste 2010*, 101–112.
- Bedin, J. Schnaid, F., Da Fonseca, A.V., & Costa Filho, L.D.M. 2012. Gold tailings liquefaction under critical state soil mechanics. *Géotechnique*, 62(3):263–267.
- Been, K. 2016. Characterizing mine tailings for geotechnical design. *Geotechnical and Geophysical Site Characterisation 5*. Australian Geomechanics Society, Sydney, Australia, 41–56.
- Been, K. & Jefferies, M.G. 1985. A state parameter for sands. Géotechnique, 35(2):99-112.
- Carrera, A., Coop, M., & Lancellotta, R. 2011. Influence of grading on the mechanical behaviour of Stava tailings. *Géotechnique*, 61(11):935–946.
- Chandler, R. J. & Tosatti, G. 1995. The Stava tailings dams failure, Italy, July 1985. *Proceedings of the Institution of Civil Engineers*, Geotechnical Engineering. 113, No. 2, 67–79.
- Cola, S., & Simonini, P. 2002. Mechanical behavior of silty soils of the Venice lagoon as a function of their grading characteristics. *Canadian Geotechnical Journal*, 39(4):879–893.
- Fourie, A. B., & Papageorgiou, G. 2001. Defining an appropriate steady state line for Merriespruit gold tailings. *Canadian Geotechnical Journal*, 38(4), 695–706.
- Fourie, A.B. & Tshabalala, L. 2005. Initiation of static liquefaction and the role of K0 consolidation. *Canadian Geotechnical Journal*, 42(3):892–906.
- Gill, S. S. 2019. Geotechnical properties of tailings: effect of fines content. University of Toronto.
- Hardin, B.O., & Richart, F.E. 1963. Elastic wave velocities in granular soils. *Journal of the Soil Mechanics and Foundations Division*, ASCE, 89(SM1):33-65.
- Jefferies, M.G., 1993. Nor-Sand: a simple critical state model for sand. Géotechnique, 43(1):91–103.
- Jefferies, M. G. & Been, K. 2015. Soil liquefaction: a critical state approach, 2nd edn. Boca Raton, FL, USA: CRC Press.
- Li, W. 2017. The mechanical behaviour of tailings. PhD. Thesis, City University of Hong Kong, Hong Kong.
- Li, W. & Coop, M.R. 2019. Mechanical behaviour of Panzhihua iron tailings. *Canadian Geotechnical Journal*, 56(3):420–435.
- Li, W., Coop, M. R., Senetakis, K., & Schnaid, F. 2018. The mechanics of a silt-sized gold tailing. *Engineering Geology*, 241, 97–108.
- Macedo, J. & Vergaray, L. 2021. Properties of Mine Tailings for Static Liquefaction Assessment. Canadian Geotechnical Journal. https://doi.org/10.1139/cgj-2020-0600.
- Macedo, J. & Petalas, A. 2019. Calibration of Two Plasticity Models against the Static and Cyclic Response of Tailings Materials. *Proceedings of Tailings and Mine Waste*. Vancouver.
- Morgenstern, N. R., Jefferies, M., Zyl, D., & Wates, J. 2019. Independent Technical Review Board. Report on NTSF Embankment Failure. Ashurst Australia.
- Morgenstern, N. R., Vick, S. G., Viotti, C. B., & Watts, B. D. 2016. Fundao tailings dam review panel. Report in the immediate causes of the failure of the Fundao Dam. New York: Cleary Gottlieb Steen and Hamilton LLP. Available at: http://fundaoinvestigation.com/the-panel-report/.
- Morgenstern, N. R., Vick, S. G., & Zyl, D. 2015. Independent Expert Engineering Investigation and Review Panel. Report on Mount Polley Tailings Storage Facility Breach. British Columbia. Available at: https://www.mountpolleyreviewpanel.ca/final-report.
- Papageorgiou, G. 2004. Liquefaction assessment and flume modelling of the merriespruit gold and bafokeng platinum tailings. PhD. Thesis University of the Witwatersrand
- Pestana, J.M. & Whittle, A.J. 1995. Compression model for cohesionless soils. *Géotechnique*, 45(4):611–631
- Rabbi, A.T.M.Z., Rahman, M.M., & Cameron, D.A. 2019. The relation between the state indices and the characteristic features of undrained behaviour of silty sand. *Soils and Foundations*, 59(4):801–813.
- Raposo, N. 2016. Deposição de rejeitados espessados. caraterização experimental e modelação numérica. PhD. Thesis, University of Porto.
- Reid, D. 2015. Estimating slope of critical state line from cone penetration test an update. *Canadian Geotechnical Journal*, 52(1), 46–57.
- Reid, D. & Fanni, R. 2020. A comparison of intact and reconstituted samples of a silt tailings. *Géotechnique*, 1–13.
- Reid, D., Fanni, R., Koh, K., & Orea, I. 2018. Characterisation of a subaqueously deposited silt iron ore tailings. *Géotechnique Letters*, 8(4), 278–283.
- Reid, D., Fourie, A., Ayala, J. L., Dickinson, S., Ochoa-Cornejo, F., Fanni, R., Garfias, A., Da Fonseca, A., Ghafghaz, M, Ovalle, C, Riemer, M, Rismanchian, A., & Suazo, G. 2020. Results of a critical state line testing round robin programme. *Géotechnique*, 1–15.
- Riemer, M. Macedo, J., Roman, O., & Paihua, S. 2017. Effects of stress state on the cyclic response of mine

- tailings and its impact on expanding a tailings impoundment. 3rd International Conference on Performance-based Design in Earthquake Geotechnical Engineering. Vancouver.
- Robertson, P.K., De Melo, L., Williams, D.J., & Wilson, G.W. 2019. Report of the Expert Panel on the Technical Causes of the Failure of Feijão Dam I.
- Sadrekarimi, A. 2013. Influence of state and compressibility on liquefied strength of sands. Canadian Geotechnical Journal, 50(10):1067–1076.
- Sadrekarimi, A. 2014. Effect of the mode of shear on static liquefaction analysis. *Journal of Geotechnical and Geoenvironmental Engineering*, 140(12):04014069.
- Sadrekarimi, A. 2016. Static Liquefaction Analysis considering principal stress directions and anisotropy. *Geotechnical and Geological Engineering*, 34(4):1135–1154.
- Sadrekarimi, A. 2020. Forewarning of Static Liquefaction Landslides. Journal of Geotechnical and Geoenvironmental Engineering, 146(9), 04020090.
- Schnaid, F., Bedin, J., Viana da Fonseca, A.J.P., & Costa Filho, L.D. 2013. Stiffness and strength governing the static liquefaction of tailings. *Journal of Geotechnical and Geoenvironmental Engineering*, 139(12):2136–2144.
- Shuttle, D.A. & Cunning, J. 2007. Liquefaction potential of silts from CPTu. *Canadian Geotechnical Journal*, 44(1):1–19.
- Shuttle, D. & Jefferies, M. 2016. Determining silt state from CPTu. Geotechnical Research, 3(3):90-118.
- Smith, K., Fanni, R., Capman, P., Reid, D. 2019. Critical State Testing of Tailings: Comparison between Various Tailings and Implications for Design. *Proceedings of Tailings and Mine Waste*. Vancouver.
- Soares, M. & Da Fonseca, A.V. 2016. Factors affecting steady state locus in triaxial tests. Geotechnical Testing Journal, 39(6):20150228.
- Yan, W. M., & Dong, J. 2011. Effect of Particle Grading on the Response of an Idealized Granular Assemblage. *International Journal of Geomechanics*, 11(4):276–285.
- Torres, L.A. 2016. Use of the cone penetration test to assess the liquefaction potential of tailings storage facilities. PhD. Thesis, University of the Witwatersrand, Johannesburg.
- USACE. 2016. National inventory of dams. Army Corp of Engineers.